Study of sorption processes and FT-IR analysis of arsenate sorbed onto red muds (a bauxite ore processing waste)

Paola Castaldi [a,*], Margherita Silvetti [a], Stefano Enzo [b], Pietro Melis [a]

[a] Dipartimento di Scienze Ambientali Agrarie e Biotecnologie Agro-Alimentari, Sez. Chimica Agraria ed Ambientale, University of Sassari, Viale Italia 39, 07100 Sassari, Italy
[b] Dipartimento di Chimica, University of Sassari, Via Vienna 2, 07100 Sassari, Italy

ARTICLE INFO

ABSTRACT

In this study we evaluated the arsenate adsorption capacity of red muds (RM), wastes tailing from the alumina production, at different pH values (4, 7, and 10). RM samples were artificially enriched in batch tests with solutions containing increasing concentrations of As(V). The pH of the solution significantly affected the adsorption, which increased with the decrease of pH. Moreover a sequential extraction procedure [H_2O; $(NH_4)_2SO_4$; $NH_4H_2PO_4$; NH_4^+-oxalate; NH_4^+-oxalate + ascorbic acid] was applied to RM samples exchanged with arsenate. Using this approach it was shown that low concentrations of arsenate sorbed in RM were present as water soluble and exchangeable fractions, while NH_4^+-oxalate and NH_4^+-oxalate + ascorbic acid extracted most of the adsorbed arsenate from RM at different pH values. Besides, FT-IR spectroscopy was used to better understand the nature of RM surface configuration after As(V) sorption. In the FT-IR spectra the presence of As(V) species was highlighted by a well resolved band at 865 cm^{-1}. The intensity and broadness of this band increased at the decreasing of pH. This band could be related to ν(As–O) vibration of an inner-sphere Al–O–As complex and/or due to As–O bonds of the adsorbed As(V) species on Fe oxides of RM samples.

© 2009 Elsevier B.V. All rights reserved.

1. Introduction

Arsenic (As) is considered among the most significant and dangerous pollutants, and is classified as human carcinogen by the International Agency for Research and Cancer (IARC). Chronic and acute poisoning by arsenic due to exposure to elevated concentrations has been reported worldwide [1].

Arsenic is generally persistent in nature, however, it can become mobile in soils so that a fraction of its total mass can leach to groundwater or become bioavailable to plants and animals.

Recently, considerable attention has been paid to the use of different types of low-cost sorbents, such as Fe/Al/Mn oxides and oxyhydroxides [2–5] zeolite and caolinite [6], laterite [7] and untreated and modified red muds [8–16] to decrease the arsenate concentration in polluted waters. Red muds (RM), among these latter one of the more promising sorbents [17,18], are fine-textured residues deriving from the digestion of bauxite during the Bayer process. These are mainly constituted by Fe, Al, Si and Ti oxides and oxyhydroxides, and tectosilicate-like compounds [19]. As a consequence, these materials could be particularly effective at blocking the arsenate in the polluted soil pore.

The ability of red muds as sorbent agents is related to their chemical, physical and structural properties [17–20]. In this sense, it is important to point out that this sorbent has a complex and variable composition which affects its reactivity [20]. An understanding of the sorption mechanism between arsenate and red muds is therefore needed to predict the long-term fate of arsenic in polluted soils treated with these sorbents. Particularly the interaction mechanisms that regulate the arsenate sorption by red muds, the mineralogical phases involved in the sorption, as well as the effects of the distribution of these compounds in soil have not been clarified yet. Specific sequential extractions of red muds exchanged with As(V), could be useful in order to predict the potential mobility of As(V), by estimating all of the chemical forms of As(V) bound to the red muds.

In this context, spectroscopic studies can also provide a deeper insight into the main phases of red muds that represent the active sites involved in the process of As(V) fixation. Because of the complicated structure of this industrial waste any spectroscopic study has not been published so far, and a significant lack of spectroscopic information about the type of interaction between red muds and arsenate sorbed exists.

The aim of this work was therefore (i) to assess, through adsorption isotherms performed under different pH conditions (pH 4, 7 and 10), the capacity of RM to interact with arsenate; (ii) to investigate, through sequential extraction, the interaction mechanisms

Table 1
Properties of the RM$_{nt}$ and RM samples at pH 10, 7 and 4 used in the study.

Chemical parameters	RM$_{nt}$	RM pH 10	RM pH 7	RM pH 4
pH	11.10	10.0	7.0	4.0
EC (mS cm^{-1})	8.70	8.25	6.55	5.22
S$_{BET}$	19.5	21.4	23.6	25.5
PCZ	4.77	–	–	–
Organic matter (% d.m.)	0.60	–	–	–
Pb (mg kg^{-1})	48.50	–	–	–
Cd (mg kg^{-1})	1.46	–	–	–
Cu (mg kg^{-1})	5.70	–	–	–
Cr (mg kg^{-1})	640.21	–	–	–
Chemical phases (wt.%)		–	–	–
Cancrinite [Na$_6$Ca$_{1.5}$Al$_6$Si$_6$O$_{24}$(CO$_3$)$_{1.6}$]	4.0	4.0	3.5	n.d.
Sodalite [Na$_8$(Cl,OH)$_2$|Al$_6$Si$_6$O$_{24}$]	20.0	24.0	24.0	22.0
Hematite [Fe$_2$O$_3$]	44.0	42.0	42.0	49.0
Boehmite [AlO(OH)]	12.0	12.0	12.0	8.0
Gibbsite [Al(OH)$_3$]	4.0	4.0	4.0	4.0
Anatase [TiO$_2$]	4.5	4.0	4.0	5.5
Andradite [Ca–Fe–Al–Si oxide]	5.5	5.0	5.0	5.5
Quartz [SiO$_2$]	6.0	5.0	5.5	6.0

that regulate the accumulation and mobility of arsenate by RM; and (iii) to determine, through Fourier transform infrared spectroscopy (FT-IR), the mineralogical phases of RM actively involved in the arsenate sorption and the types of surface complex formed through sorption of arsenate on RM.

2. Materials and methods

2.1. Sample description

Red muds were obtained from the Eurallumina plant (Portovesme, Sardinia, Italy). The red muds were dried overnight at 105 °C, finely ground and sieved to <0.02 mm (RM$_{nt}$). The pH and electric conductivity (EC) values were determined in 1:25 ratio of red mud/distilled water (Table 1) [19]. The specific surface area of the RM$_{nt}$ was determined by applying the BET model to the N$_2$ adsorption results obtained from a Sorptomatic Carlo Erba (Milan, Italy). The samples were also pre-treated by outgassing at 40 °C combined with vacuum at 10^{-9} bar for 12 h. The error in the determination of SBET was ±3 m^2 g^{-1}.

Total organic matter in the RM was determined using the method of Walkley and Black described in the paper of Garau et al. [17]. The total concentration of selected heavy metals in RM$_{nt}$ samples was determined by drying the red mud overnight at 105 °C and digesting it with HNO$_3$ and HCl (ratio 1/3) in a Microwave Milestone MLS 1200. The heavy metal concentrations were determined using a PerkinElmer Analyst 600 atomic absorption spectrometer (FAAS) equipped with HGA graphite furnace.

X-ray diffraction (XRD) analysis of RM$_{nt}$ at pH 4, 7 and 10 was carried out with a Rigaku D/MAX diffractometer (Cu Kα) equipped with a graphite monochromator in the diffracted beam. The pattern was collected in the 2θ range from 10° to 70°. Crystalline phases were identified using the database of the International Centre for Diffraction Data for Inorganic Substances (Table 1) [20]. Aside from crystalline phases, about the 20% of the RM was made of amorphous oxides.

The pH$_{PZC}$ of the RM$_{nt}$ samples was measured by Laser Doppler Velocimetry coupled with Photon Correlation Spectrometry using a Coulter Delsa 440 spectrometer equipped with a 5 mW He–Ne laser (632.8 nm) [20].

2.2. Adsorption and release through sequential extraction of As(V) from RM samples

All chemicals were of analytical grade and used without further purification. RM$_{nt}$ samples were artificially enriched with

solutions containing increasing concentrations of Na$_2$HAsO$_4$·7H$_2$O to obtain adsorption isotherms. Three batch experiments were prepared at three pH values (4, 7 and 10) and at constant temperature (25 ± 1 °C). Polyethylene bottles containing 1.0 g of red muds were filled with 25 mL of arsenate enriched solutions. Particularly 15 points on the whole were obtained to create the adsorption isotherm, corresponding to the addition of different volume of 0.2 M Na$_2$HAsO$_4$·7H$_2$O solution. The concentration of Na$_2$HAsO$_4$·7H$_2$O added to 1.0 g of red muds varied between 8 × 10^{-4} and 0.18 M (which correspond to 0.02 and 4.5 mmol 25 mL^{-1}, respectively). A background electrolyte of 0.1 M NaCl was used as diluent for all batch experiments. The pH values of the mixtures RM/polluting solution were adjusted with either HCl or NaOH solutions, the concentration of which were 0.01, 0.1 and 1.0 M. The mixtures (1:25 ratio of red mud/As(V) solution) were shaken for 24 h at constant temperature (25 ± 1 °C). After equilibrium, the samples were centrifuged at 8000 rpm for 10 min and filtered to completely separate the liquid and solid phases. An aliquot of the supernatant was taken and analyzed. As(V) was measured by ionic chromatography by using an IonPac AS12A Analytical Column equipped with an IonPac AG12A Guard Column, 4 mm. Carbonate 2.1 mM/bicarbonate 0.8 mM was employed as the eluent at a flow rate of 1.5 mL/min. The sample loop valve was 10 μL.

The concentration of As(V) in the final enriched RM samples (reported in the x-axis of Fig. 1) was also determined to verify that the total content of arsenate (supernatants + final enriched RM) actually corresponded to the arsenate added to RM. The solid phase of RM deriving from each point of the isotherms was dried overnight at 105 °C and digested with 65% HNO$_3$ + 30% H$_2$O$_2$ in a Microwave Milestone MLS 1200. The As(V) concentration was measured by ionic chromatography as described above. The sum of As(V) concentration in the supernatant and in the final enriched RM was not significantly different, at the 95% confidence limit with respect to the As(V) concentration added in each RM samples. Each experiment was conducted in triplicate and mean values were reported.

The chemical forms of the arsenate bound to the red muds were determined by a sequential extraction procedure [21], in order to study the contribution of the different interaction mechanisms. RM samples (1 g) saturated with arsenate at pH 4, 7 and 10, deriving from the last point of the isotherms, were placed in 50 mL centrifugation tubes and treated with 25 mL of distilled water (pH 6.5) and shaken for 2 h at room temperature to extract the As(V) soluble (Step 0). These samples were then treated with 25 mL of 0.05 M (NH$_4$)$_2$SO$_4$ and shaken for 4 h at 20 °C to extract the As(V) non-specifically sorbed (Step 1). The same RM samples were then
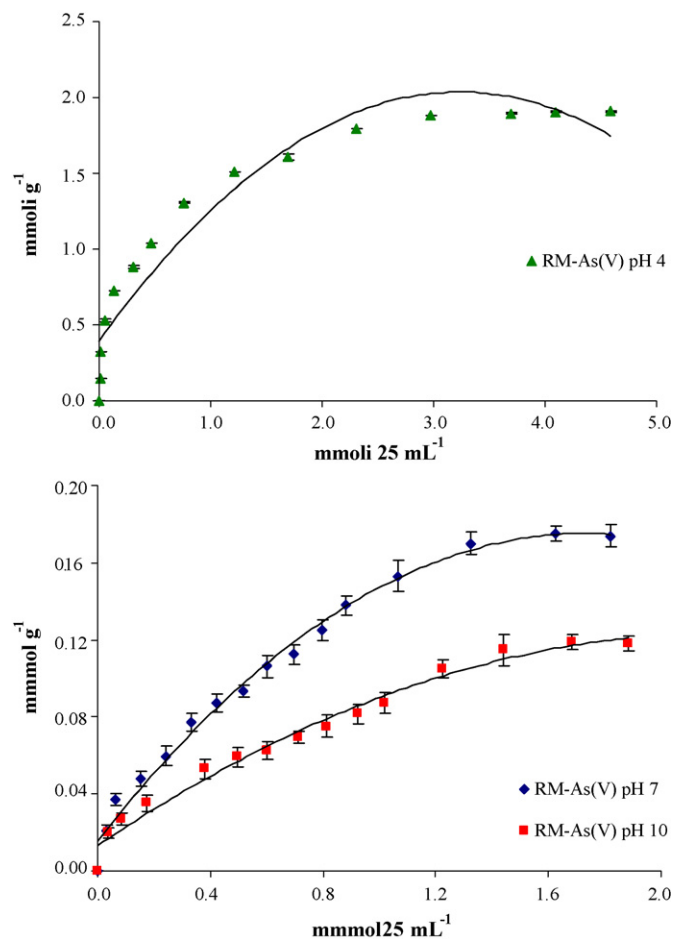
Fig. 1. As(V) adsorption isotherms on RM samples at different pH values.

treated with 25 mL of 0.05 M $NH_4H_2PO_4$ and shaken for 16 h at 20 °C to extract the As(V) specifically sorbed (Step 2). They were then treated with 25 mL of 0.2 M NH_4^+-oxalate buffer (pH 3.25) and shaken for 4 h in the dark at 20 °C to extract the As(V) associated with amorphous and poorly crystalline hydrous oxides of Fe and Al (Step 3) and with 25 mL of 0.2 M NH_4^+-oxalate buffer + 0.1 M ascorbic acid (pH 3.25) and shaken for 0.5 h in a water basin at 96 °C ($\pm$3) in the light to extract the As(V) associated with well-crystallized hydrous oxides of Fe and Al (Step 4).

After each step of the extraction process the RM samples were centrifuged at 8000 rpm for 10 min and filtered to separate the liquid and solid phases. After the fifth washing, the residual fraction of As(V) was determined by drying the solid phase overnight at 105 °C and digesting it with 65% HNO_3 + 30% H_2O_2 in a Microwave Milestone MLS 1200. The As(V) concentration was measured by ionic chromatography as described above. The sum of As(V) concentration determined in the supernatant after each extraction step and that present in the final enriched RM was not significantly different at the 95% confidence limit with respect to the As(V) concentration in RM samples saturated with arsenate. The residual fraction discussed in the text is this determined after the RM total dissolution.

Each step of the sequential extraction procedure at the three pH values was carried out in triplicate and the mean values were reported.

2.3. X-ray fluorescence (XRF) spectroscopy

XRF-measurements of RM samples exchanged with As(V) at pH 4, 7 and 10 were carried out by using a portable equipment com-

posed of an X-ray tube (molybdenum anode, Oxford Instruments) working at 25 kV and 0.1 mA. An aluminum collimator 1 cm long and with an internal hole 1 mm in diameter permits to irradiate an area of about 0.2 cm² of the object to be analysed, at a distance tube window-sample of about 2 cm. A Si-PIN detector from AMPTEK was employed with a thickness of about 300 mm and characterized by an energy resolution of about 200 eV at 5.9 keV.

2.4. FT-IR spectroscopy

The FT-IR spectra were recorded at room temperature using a Nicolet 380 FT-IR spectrometer equipped with EZ Omnic software. The FT-IR spectra were recorded in the 4000 to 400 cm⁻¹ range, and were collected after 256 scans at 4 cm⁻¹ resolution. The KBr disc technique was used for sample preparation. The KBr (FT-IR grade, Fluka) was dried at 200 °C for 24 h. To prepare KBr pellets, 1 mg of RM sample (deriving from the RM–As(V) samples at pH 4, 7 and 10 of the last point of isotherms, and coming from the extraction procedure steps of RM–As(V) samples at pH 4) was ground 1–2 min together with 200 mg of KBr. The pellets were made using 90 mg of the mixture KBr–RM. This latter was pressed in a dye under vacuum for 4–6 min at 12t pressure to produce transparent disks about 1 mm thick and 13 mm in diameter. An empty KBr pellet was used as reference and its spectrum was subtracted from the sample spectrum to suppress spectral artifacts caused by KBr impurities and water.

3. Result and discussion

3.1. Characteristics of the sorbent

Table 1 shows the properties of the RM samples at different pH values used in the study. The specific areas of RM at pH 4, 7 and 10 were 25.5, 23.6 and 21.4 m² g⁻¹, respectively. A mixture of eight phases was retrieved in RM_{nt} samples, however it should be noted that the 60 wt.% of the RM sample was made by Fe and Al oxide and oxyhydroxides as hematite (ICSD #15840, S.G.R-3 c H, $a = 0.5038$ nm, $c = 1.3772$ nm), boehmite (ICSD #10-0391, Cmcm, $a = 0.287$ nm, $b = 1.223$ nm, $c = 0.370$ nm) and gibbsite (ICSD #6-162, P21/C, $a = 0.870$ nm, $b = 0.487$ nm, $c = 0.969$ nm) (Table 1). Besides, XRD analysis showed that the different pH values changed the mineralogical composition of RM. In addition to this and with obvious cautions suggested by the uncertainties of the quantitative determination, the percentage of boehmite decreased at pH 4 (Table 1). Also the cancrinite phase disappeared on decreasing the pH and sodalite percentage was higher (24 wt.%) in RM samples at pH 7 and 10 (Table 1).

3.2. Adsorption Isotherms of As(V) on RM at different pH values

The effects of the solution pH on arsenate sorption in red muds were studied by varying the pH of the solution over a range of 4–10.

The adsorption isotherms obtained were regular, positive, and concave to the concentration axis and a plateau was reached in all three curves (Fig. 1). The arsenate sorption decreased with increased in adsorbate concentration, which indicated that the adsorption depended upon the availability of the binding sites for arsenate [19].

Isotherm analyses showed that different concentrations of arsenate were sorbed at different pH values. These latter affected both the surface charge of the solid particles and the degree of ionization and speciation of anionic specie. Particularly the As(V) sorption was higher at lower pH values and increased in the following order: RM–As(V) pH 4 (1.908 mmol g⁻¹) > RM–As(V) pH 7 (0.174 mmol g⁻¹) > RM–As(V) pH 10 (0.118 mmol g⁻¹) (Fig. 1). The arsenate sorbed by the RM at pH 4 was 11.0 and 16.2 times higher

Table 2
The Langmuir parameters b and K, relating to the As(V) adsorption capacity and intensity of RM at different pH values.

	b (mmol g^{-1})	K (L mmol^{-1})	R^2
RM–As(V) pH 4	1.83	0.94	0.99
RM–As(V) pH 7	0.17	2.45	0.85
RM–As(V) pH 10	0.12	4.55	0.94

compared to that sorbed into RM at pH 7 and 10, respectively. This sorption behaviour was similar to the effect of the pH on arsenic adsorption on RM modified with FeCl$_3$ [16], seawater neutralized red mud [13] and acid treated red mud [12].

The arsenate sorption on red mud surfaces at different pH values could be attributed to various mechanisms, such as electrostatic attraction/repulsion, chemical interaction and ion exchange [22]. The pH dependence of As sorption by red muds can be further understood by considering the point of zero surface charge (pH$_{pzc}$) of red muds, which was 4.77. The pH$_{pzc}$ is where the surface charge switches from negative at higher pH$_{pzc}$ to positive at lower pH$_{pzc}$ values. However, the transition from dominantly negative surface charges on the constituent particles in RM to dominantly positive charges will be much more gradual than for pure minerals [9]. At pH 4.0 arsenate mainly exists as H$_2$AsO$_4^-$ anion and adsorption in RM is facilitated by electrostatic attraction, as the surface of red muds is positively charged. Besides, at this pH value the presence of fewer OH$^-$ ions, that can compete with the arsenate anions for the available sorption sites, is supposed. On the other hand, at pH 10.0, where the divalent anion HAsO$_4^{2-}$ dominates, and at pH 7, where both species co-exist (H$_2$AsO$_4^-$ and HAsO$_4^{2-}$), generally the surface of the solid is negatively charged and the arsenate may be affected by Coulombic repulsion [9] and could compete with an higher concentration of hydroxide ions for positively charged surface sites. The lower adsorption capacities found at higher pH values were probably due to the decrease of positively charged surface sites in RM, therefore the arsenate sorption should be mainly due to chemical sorption of specific anions [13,14], which involved the incorporation of anions as a ligands in the coordination shell of the sorbent [2,15].

However the red muds are a complex mixture of minerals, each characterized by a different point of zero surface charge value. For example, the pH$_{pzc}$ value of hematite is about 8.1, whereas the pH$_{pzc}$ of gibbsite and boehmite are about 9.4 and 8.6 respectively [22]. The fact that the As(V) sorption in RM was higher at pH 7.0 than pH 10 could be due to positive charge of oxyhydroxides of Al and a partial positive charge of hematite, since the change from a strongly positive to a strongly negative zeta potential takes place gradually over 1.5–2 pH units [13].

For the present study the Langmuir model, which is the simplest and most commonly used model that assumes monolayer adsorption [15], was employed. The Langmuir equation was applied for adsorption equilibrium as follows:

$$\frac{x}{m} = \frac{KbC}{1 + KC}$$

the Langmuir parameter b refers to maximum adsorption capacity and K is a proportional constant of the adsorption energy [23,24]. In this study, the high correlation coefficients indicated that the Langmuir isotherm fits the adsorption data (Table 2). The maximum adsorption capacity values of arsenate, obtained from the Langmuir's equation, agreed with the experimental results (Table 2). The maximum As(V) adsorption b in RM at pH 4 was in fact higher than As(V) adsorption b at pH 7 and 10.

Since the inner-sphere complexes are much stronger than outer-sphere complex bonds, and the inner-spherically adsorbed arsenic anions are not considered to be readily exchangeable, it
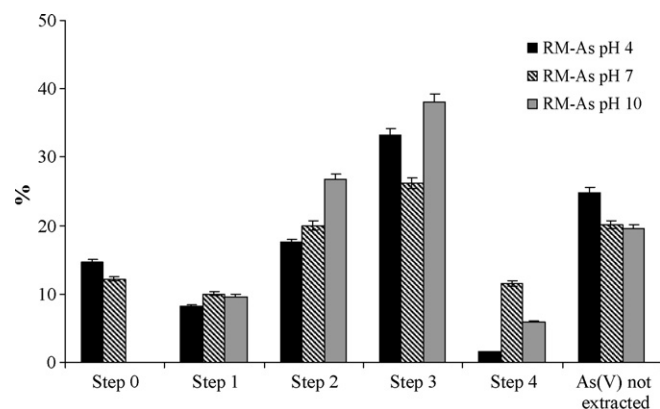

Fig. 2. Percentage of As(V) extracted with H$_2$O (Step 0); (NH$_4$)$_2$SO$_4$ (Step 1); NH$_4$H$_2$PO$_4$ (Step 2); NH$_4^+$-oxalate (Step 3) NH$_4^+$-oxalate buffer + ascorbic acid (Step 4), and not extracted from RM–As(V) at different pH values.

is possible to hypothesize that arsenate sorbed in RM at pH 10, despite a superficial electrostatic repulsion, mainly establishes strong bonds. This assumption was supported by the Langmuir's parameter K which showed the highest values for the RM–As(V) pH 10 (4.55 L mmol^{-1}) followed by RM–As(V) pH 7 (2.44 L mmol^{-1}) and RM–As(V) pH 4 (0.94 L mmol^{-1}).

3.3. Sequential extraction on RM samples exchanged with As(V) at different pH values

The red mud samples exchanged with arsenate, were treated with solutions of gradually increasing extraction strength [21], in order to study the different arsenate–red muds interaction mechanisms.

The fractions extracted with H$_2$O, which are associated with the greater environmental hazard being the most soluble and bioavailable fractions, were less than 15% of the arsenate adsorbed in RM samples and followed the order RM–As(V) pH 4 > RM–As(V) pH 7 > RM–As(V) pH 10. Particularly in RM samples at pH 10 no fractions of arsenate extracted with H$_2$O were detected (Fig. 2). The percentage of arsenate extracted with (NH$_4$)$_2$SO$_4$, which are associated with the relatively labile exchangeable fractions, particularly with As(V) bounded through outer-sphere complex, increased as pH decreased. The percentage of arsenate extracted with NH$_4$H$_2$PO$_4$, which represent the As(V) specifically sorbed [21], were higher in RM at pH 10. Also the percentage of arsenate extracted with oxalate and ascorbic acid (Steps 3 and 4), which were associated with amorphous, poorly crystalline and well-crystallized oxides and oxyhydroxides of Fe and Al [21], increased with increasing of pH. These two fractions were higher than 36% of the arsenate adsorbed in all the RM samples. The fractions of non-extracted As(V) would not be expected to be readily released under natural conditions. The residual fractions of As(V) in RM at pH 4, 7 and 10 were respectively the 25, 20 and 19% of the arsenate adsorbed (Fig. 2).

The results of the sequential extraction procedure showed that in RM samples low quantities of As(V) were as water-soluble and exchangeable fractions. Particularly it was possible to believe that about the 20% of As(V) was physically sorbed in RM at pH 4, as a consequence of the electrostatic attraction between the positive charge of the red mud surface and the negative charge of the anion. By contrast, in RM at pH 10 more than 90% of arsenate associated was chemically sorbed. The main mechanism governing the adsorption process probably involved the formation of inner-sphere surface complexes and/or much stronger forces comparable to those leading to the formation of chemical compounds in which the As(V) is incorporated as a structural component of low-solubility miner-
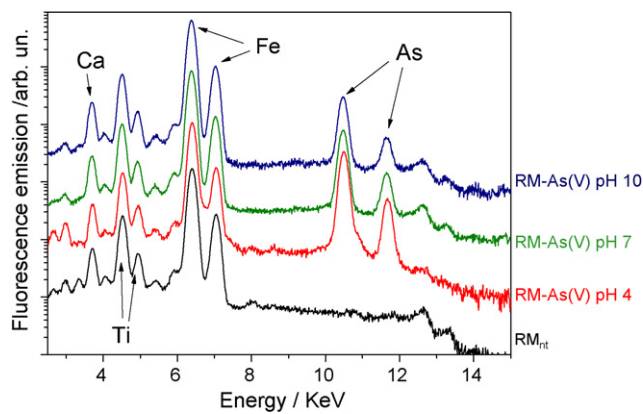
Fig. 3. XRF spectra of RM$_{nt}$ and RM–As(V) at different pH values.

als (e.g., calcium iron arsenates or calcium aluminum arsenates). Therefore, once bound to the red muds surface, the As(V) at pH 10 should remain trapped and no more soluble or physically exchangeable.

3.4. X-ray fluorescence (XRF) analysis

Fig. 3 shows the fluorescence spectra of RM$_{nt}$ and RM samples exchanged with As(V) at different pH values. With respect to untreated RM, where emission doublets typical of Ca, Ti, Fe elements can be easily recognized, the As doublet was evident in the RM doped with arsenate. From analysis of the relative intensities of emission line it seems that the higher the pH, the lower the amount of adsorbed As, as highlighted by the adsorption results.

3.5. FT-IR spectra analysis

The nature of RM surface configuration after As(V) sorption was evaluated by spectroscopic analyses. FT-IR spectra of arsenate sorbed to the RM samples at pH 4, 7 and 10 are shown in Fig. 4. The spectra interpretation was complicated because of the complex composition of red muds due to the presence of several mineralogical phases containing numerous adsorption sites. In all of the spectra a strong band was present in the hydroxyl stretching region at 3400–3300 cm^{-1}. This was likely due to the presence of H$_2$O in the red muds [20,25]. In the spectra a band at 3090 cm^{-1} was also visible. This band, which could be ascribed to O–H stretching vibration of crystalline boehmite [26], increased its intensity as the pH increased. This results is consistent with that obtained from XRD analyses of RM at pH 4, where a decrease of boehmite was observed. Besides, the band at 3090 cm^{-1} was poorly resolved in RM–As(V) at pH 4 and the losing of this signal could provide both evidence for an As(V)-surface direct bonding with the boehmite phase of red mud, than the formation of aluminum arsenate precipitates.

In all the samples a band at 1630 cm^{-1} was detected. This was attributed to the water molecules occluded inside the aluminosilicate structure [20]. Carbonates bands appear in the RM samples at pH 7 and 10, within the 1410–1470 cm^{-1} region, while these bands were missing in the RM samples at pH 4. The peak recorded at 1400 cm^{-1} in all the samples could be attributed to nitrate, this NO$_3$$^-$ band could be present in both cancrinite and sodalite, according with the results reported by Zhao et al. [27]. The peak at 1070 cm^{-1} in the RM at pH 4, which was a shoulder in the RM samples at pH 7 and 10, is characteristic of a band corresponding to Si–O vibration [28]; alternatively, as showed by Goldberg and Johnston [2] it could be attributed to a carbonate band. The band at 994 cm^{-1} present in RM samples could be assigned to the stretching vibrations of Si(Al)–O. This band is sensitive to the content of structural
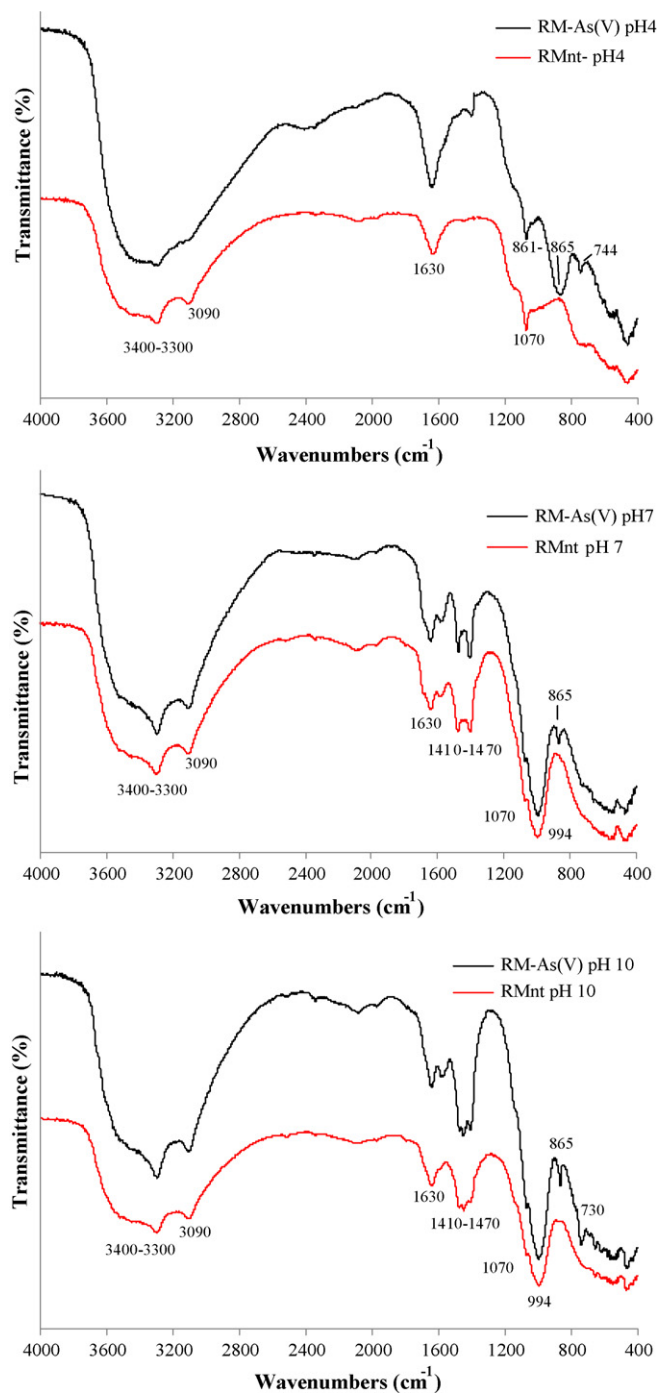

Fig. 4. FT-IR spectra of RM$_{nt}$ and RM–As(V) at different pH values.

Si and Al [29]. The disappearance of this band in RM samples at pH 4 could be due to dissolution of cancrinite with acid treatment, as demonstrated by XRD analyses (Table 1).

The infrared spectral band, due to As–O stretching vibrations of the adsorbed arsenate species, appeared to contain a main component. There was a well resolved band which peaks at 861–865 cm^{-1} and its intensity and broadness increased as the pH decreased from 10 to 4. This band could be related to ν(As–O) vibration of an inner-sphere Al–O–As complexes and/or could be also due to As–O bonds of the adsorbed As(V) species on Fe oxides [2,30]. The lack of pH dependence on the positions of the ν(As–O) modes and the similarity of the band position at 861–865 cm^{-1} in RM–As(V) at pH 4, 7 and 10 suggested that these interactions are "protected" from
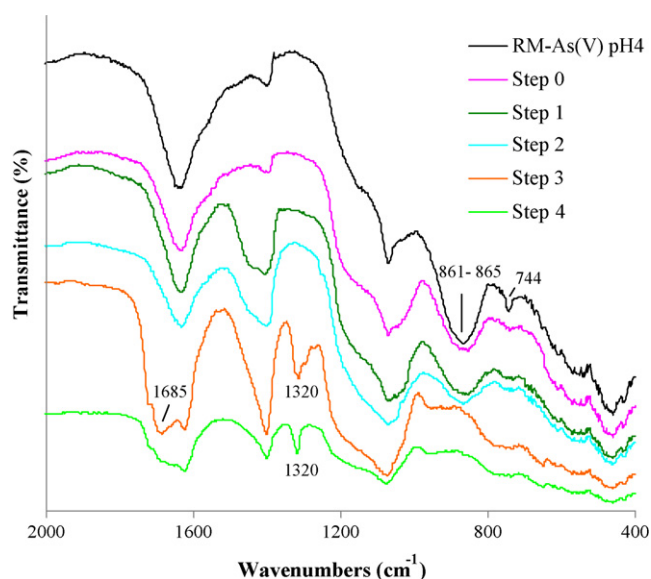
Fig. 5. FT-IR spectra of RM–As(V) at pH 4 after the sequential extraction steps.

the pH changes, indicating that a similar mechanism of arsenate sorption occurred. Probably the arsenate groups were involved in a direct inner-sphere complexation with the Al and/or Fe surface phases of RM. Besides, as suggested also by Myneni et al. [31], the vibrational spectra of arsenate adsorbed on Fe oxides of RM overlapped with those of arsenate adsorbed on Al-oxides and oxyhydroxides, which exhibited the same peaks in the region of interest. Finally, according with the results reported by Myneni et al. [31] and Roddick-Lanzillotta et al. [32] it was difficult to determine the type of coordination from the spectra of the adsorbed arsenate because both protonated and unprotonated anions were present.

As previously mentioned, in the RM–As(V) at pH 4 there was a broad band, which peaks at 861–865 cm^{-1}, and which covered the region between 940 and 800 cm^{-1}. This broad band could have obscured some other peaks. For examples as reported by several authors a peak at 878–880 cm^{-1} could be assigned to uncomplexed asymmetric As–O stretching vibration [30–33]. The presence of uncomplexed As–O in the RM–As(V) at pH 4 could be due to electrostatic attraction, as the red muds surface was positively charged at pH 4. Therefore the nature of the arsenate complexation schemes in RM at pH 4 was difficult to evaluate exclusively with the FT-IR spectra information.

A distinct peak at 744 cm^{-1} in RM–As(V) at pH 4 was also visible, and could be assigned to symmetric stretching vibrations of As–O–Al [2,31]. The band at 730 cm^{-1} in the RM–As(V) at pH 10 could be assigned to As–O ν_s of arsenate sorbed into Fe oxyhydroxides as pointed out by Lumdson et al. [34], which reported a similar band in the IR spectra of AsO$_4^{3-}$ adsorbed on goethite.

The peaks detected in the region within 400–500 cm^{-1} of all the RM samples could be due to the T–O bend (where T corresponds to Si or Al) of sodalite and cancrinite structure [20]. Also in the region 560–630 cm^{-1} the peaks detected could be due to 4- or 6-membered rings vibrations of SiO$_4$ or AlO$_4$ tetrahedra [20]. Moreover, in all the RM spectra a peak due to stretching vibrations of Fe–O bond (460–500 cm^{-1} range) was also present [25].

To better understand the interaction between As(V) and RM at pH 4, FT-IR analyses of RM–As(V) samples were performed after each sequential extraction step (Fig. 5). The band which peaks at 861–865 cm^{-1} was progressively more and more flattened as the extraction steps proceeded until to disappear after the extraction with NH$_4^+$-oxalate (Step 3), which quantified the As(V) sorbed

into amorphous and poorly crystalline oxides and oxyhydroxides of Fe and Al (Fig. 5). By contrast, a strong decrease of peak at 744 cm^{-1} was observed after the extraction steps 0 and 1 (extraction with water and (NH$_4$)$_2$SO$_4$), showing that this peak indicated an unspecific electrostatic interaction between As(V) and Al-phases of red muds. After the extraction with NH$_4$H$_2$PO$_4$ (Step 2), the band between 940 and 800 cm^{-1} was considerably flattened than RM–As(V) and the peak at 865 cm^{-1} still evident. Therefore the extraction with phosphate, which is an anion that compete for the same adsorption sites of arsenate, probably did not exchange all the As(V) inner-sphere complexed. Besides, in the spectrum of Step 2 the expected bands associated with P–O(H) stretching vibrations, which are in the 800–1250 cm^{-1} region, were lacking [35] (Fig. 5), indeed in this region the bands present were the same observed in the Step 1 spectrum (extraction with (NH$_4$)$_2$SO$_4$). The spectrum of Step 3 showed new bands at 1320 cm^{-1} (also visible in the Step 4 spectrum) and at 1685 cm^{-1}, which were assigned respectively to C=O stretching vibrations of outer-sphere adsorption of oxalate [36] and to the νC=O stretches originating from the Fe-oxalate formed [37–38].

4. Conclusions

The sorption properties of the RM used in this study were significantly influenced by the pH, which affected both the surface charge of the solid particles than the degree of ionization and speciation of arsenate species. The interaction mechanisms between As(V) and red muds were of several type: electrostatic attraction/repulsion, chemical interaction and ion exchange. The arsenate sorption in RM samples increased as the pH decreased from 10 to 4. This could be due to the formation of chemical bonds, and to unspecific electrostatic bonds between RM at pH 4 and arsenate, since at this pH value the red mud surfaces were positively charged. Besides, the results of sequential extraction showed that a higher percentage of As(V) in RM at pH 4 was exchanged with H$_2$O and (NH4)$_2$SO$_4$ with respect to that extracted in RM at pH 7 and 10. Therefore it was possible to hypothesize that the As(V) in RM at pH 7 and 10 was mainly sorbed through a ligand exchange mechanism that involved the formation of inner-sphere complexes. However, it should be taken into account that the absolute total As content in RM enriched at pH 4 is much higher than at pH 7 and 10, and therefore also the absolute value which remains adsorbed after the extraction with water and (NH4)$_2$SO$_4$ is higher than that obtained in the case of RM–As(V) at pH 7 and 10.

The FT-IR spectra of RM–As(V) showed that the oxides and oxyhydroxides of Fe and Al (hematite, boehmite and gibbsite) of RM were probably the mineralogical phases involved in the sorption processes. However, this spectroscopic technique did not discriminate the different role of Fe–Al oxides and oxyhydroxides in the arsenate polyhedra sorption. At the same time it was difficult to determine the type of coordination of the As(V) adsorbed because both protonated and unprotonated arsenate ions were present. The infrared band due to adsorbed arsenate species was at 861–865 cm^{-1} and its intensity and broadness increased as the pH decreased, because of the higher As(V) sorption at pH 4. After the sequential extraction steps FT-IR spectra of RM–As(V) at pH 4 showed that the band at 865 cm^{-1} was completely disappeared after the extraction with NH$_4^+$-oxalate. Consequently, in agreement with the results of the sequential extraction, it is concluded that most of As(V) sorbed in RM (about the 80%) was strongly and specifically associated with the Fe–Al oxides and oxyhydroxides phases.

The results obtained showed that the adsorbing properties of red muds are related with their capacity to decrease the mobility of the arsenate through exchange reactions. These aspects are

of particular importance in order to evaluate the efficiency of the red muds as As-sorbents in polluted soils which have different pH values.

References

[1] S. Wang, C.N. Mulligan, Speciation and surface structure of inorganic arsenic in solid phases: a review, Environ. Int. 34 (2008) 867–879.
[2] S. Goldberg, C.T. Johnston, Mechanisms of arsenic adsorption on amorphous oxides evaluated using macroscopic measurements, vibrational spectroscopy, and surface complexation modeling, J. Colloid Interface Sci. 234 (2001) 204–216.
[3] C. Luengo, M. Brigante, M. Avena, Adsorption kinetics of phosphate and arsenate on goethite. A comparative study, J. Colloid Interface Sci. 311 (2007) 354–360.
[4] T.P. Luxton, M.J. Eick, D.J. Rimstidt, The role of silicate in the adsorption/desorption of arsenite on goethite, Chem. Geol. 252 (2008) 125–135.
[5] A. Violante, M. Pucci, V. Cozzolino, J. Zhu, M. Pigna, Sorption/desorption of arsenate on/from Mg–Al layered double hydroxides: influence of phosphate, J. Colloid Interface Sci. 333 (2009) 63–70.
[6] Z. Li, R. Beachner, Z. McManama, H. Hanlie, Sorption of arsenic by surfactant-modified zeolite and caolinite, Micropor. Mesopor. Mater. 105 (2007) 291–297.
[7] F. Partey, D.I. Norman, S. Ndur, R. Nartey, Mechanism of arsenic sorption onto laterite iron concretions, Colloid Surf. A 337 (2009) 164–172.
[8] H.S. Altundoğan, S. Altundoğan, F. Tűmen, M. Bildik, Arsenic removal from aqueous solutions by adsorption on red mud, Waste Manage. 20 (2000) 761–767.
[9] H. Genç-Fuhrman, J.C. Tjell, D. McConchie, Adsorption of arsenic from water using activated neutralized red mud, Environ. Sci. Technol. 38 (2004) 2428–2434.
[10] H. Genç-Fuhrman, H. Bregnhoj, D. McConchie, Arsenate removal from water using sand–red mud columns, Water Res. 13 (2005) 2944–2954.
[11] H. Genç-Fuhrman, J.C. Tjell, D. McConchie, Increasing the arsenate adsorption capacity of neutralized red mud (Bauxsol), J. Colloid Interface Sci. 271 (2004) 313–320.
[12] H.S. Altundoğan, S. Altundoğan, F. Tümen, M. Bildik, Arsenic adsorption from aqueous solutions by activated red mud, Waste Manage. 22 (2002) 357–363.
[13] H. Genç, J.C. Tjell, D. McConchie, O. Schuiling, Adsorption of arsenate from water using neutralized red mud, J. Colloid Interface Sci. 264 (2003) 327–334.
[14] P.B. Bhakat, A.K. Gupta, S. Ayoob, S. Kundu, Investigations on arsenic(V) removal by modified calcined bauxite, Colloids Surf. A 281 (2006) 237–245.
[15] D. Mohapatra, D. Mishra, K.H. Park, A laboratory scale study on arsenic(V) removal from aqueous medium using calcined bauxite ore, J. Environ. Sci. (2008) 683–689.
[16] S. Zhang, C. Liu, Z. Luan, X. Peng, H. Ren, J. Wang, Arsenate removal from aqueous solutions using modified red mud, J. Hazard. Mater. 152 (2008) 486–492.
[17] G. Garau, P. Castaldi, L. Santona, P. Deiana, P. Melis, Influence of red mud, zeolite and lime on heavy metal immobilization, culturable heterotrophic microbial populations and enzyme activities in a contaminated soil, Geoderma 142 (2007) 47–57.
[18] P. Castaldi, P. Melis, M. Silvetti, P. Deiana, G. Garau, Influence of pea and wheat growth on Pb, Cd, and Zn mobility and soil biological status in a polluted amended soil, Geoderma 151 (2009) 241–248.
[19] L. Santona, P. Castaldi, P. Melis, Evaluation of the interaction mechanisms between red muds and heavy metals, J. Hazard. Mater. 136 (2006) 324–329.
[20] P. Castaldi, M. Silvetti, L. Santona, S. Enzo, P. Melis, XRD, FT-IR, and thermal analysis of bauxite ore-processing waste (red mud) exchanged with heavy metals, Clay. Clay Miner. 56 (2008) 461–469.
[21] W.W. Wenzel, N. Kirchbaumer, T. Prohaska, G. Stingeder, E. Lombi, D.C. Adriano, Arsenic fractionation in soils using an improved sequential extraction procedure, Anal. Chim. Acta 436 (2001) 309–323.
[22] Y. Li, C. Liu, Z. Luan, X. Peng, C. Zhu, Z. Chen, Z. Zhang, J. Fan, Z. Jia, Phosphate removal from aqueous solutions using raw and activated red mud and fly ash, J. Hazard. Mater. 137 (2006) 374–383.
[23] K. Periasamy, C. Namasivayam, Process development for removal and recovery of cadmium from wastewater by a low cost adsorbent: adsorption rates and equilibrium studies, Ind. Eng. Chem. Res. 33 (1994) 317–320.
[24] P. Castaldi, L. Santona, S. Enzo, P. Melis, Sorption processes and XRD analysis of a natural zeolite exchanged with Pb^{2+}, Cd^{2+} and Zn^{2+} cations, J. Hazard. Mater. 156 (2008) 428–434.
[25] H.D. Ruan, R.L. Frost, J.T. Kloprogge, The behavior of hydroxyl units of synthetic goethite and its dehyxylated product hematite, Spectrochim. Acta 57 (2001) 2575–2586.
[26] A. Boumaza, L. Favaro, J. Lédion, G. Sattonnay, J.B. Brubach, P. Berthet, A.M. Huntz, P. Roy, R. Tétot, Transition alumina phases induced by heat treatment of boehmite: an X-ray diffraction and infrared spectroscopy study, J. Solid State Chem. 182 (2009) 1171–1176.
[27] H.T. Zhao, Y.J. Deng, J.B. Harsh, M. Flury, J.S. Boyle, Alteration of caolinite to cancrinite and sodalite by simulated Hanford tank waste and its impact on cesium retention, Clay. Clay Miner. 52 (2004) 1–13.
[28] A. Gök, M. Omastová, J. Prokeš, Synthesis and characterization of red mud/polyaniline composites: electrical properties and thermal stability, Eur. Polym. J. 43 (2007) 2471–2480.
[29] P. Castaldi, L. Santona, C. Cozza, V. Giuliano, C. Abbruzzese, V. Nastro, P. Melis, Thermal and spectroscopic studies of zeolites exchanged with heavy metals cations, J. Mol. Struct. 734 (2005) 99–105.
[30] Y. Jia, L. Xu, X. Wang, G.P. Demopoulos, Infrared spectroscopic and X-ray diffraction characterization of the nature of adsorbed arsenate on ferrihydrite, Geochim. Cosmochim. Acta 71 (2007) 1643–1654.
[31] S.C.B. Myneni, S.J. Traina, G.A. Waychunas, T.J. Logan, Experimental and theoretical vibrational evaluation of arsenate coordination in aqueous solutions, solids, and at mineral–water interface, Geochim. Cosmochim. Acta 62 (1998) 3285–3300.
[32] A.J. Roddick-Lanzillotta, A.J. McQuillan, D. Craw, Infrared spectroscopic characterization of arsenate(V) ion adsorption from mine waters, Macraes, mine, New Zealand, Appl. Geochem. 17 (2002) 445–454.
[33] L. Jing, Z. Fenghua, Characterization of arsenate adsorption on amorphous Al gels with Keggin structure by Fourier transformed infrared spectroscopy and MAS 27Al NMR, Chin. J. Geochem. 28 (2009) 61–69.
[34] D.G. Lumsdon, A.R. Fraser, J.D. Russell, N.T. Livesey, New infrared band assignments for the arsenate ion adsorbed on synthetic goethite (α-FeOOH), J. Soil Sci. 35 (1984) 381–386.
[35] P. Persson, N. Nilsson, S. Sjöberg, Structure and bonding of orthophosphate ions at the iron oxide–aqueous interface, J. Colloid Interface Sci. 177 (1996) 263–275.
[36] S.J. Hug, D. Bahnemann, Infrared spectra of oxalate, malonate and succinate adsorbed on the aqueous surface of rutile, anatase and lepidocrocite measured with in situ ATR-FTIR, J. Electron Spectrosc. 150 (2006) 208–219.
[37] K. Axe, M. Vejgården, P. Persson, An ATR-FTIR spectroscopic study of the competitive adsorption between oxalate and malonate at the water–goethite interface, J. Colloid Interface Sci. 294 (2006) 31–37.
[38] A. Nevin, J.L. Melia, I. Osticioli, G. Gautier, M.P. Colombini, The identification of copper oxalates in a 16th century Cypriot exterior wall painting using micro FTIR, micro Raman spectroscopy and gas chromatography–mass spectrometry, J. Cult. Herit. 9 (2008) 154–161.